# Molecular Hexanuclear Clusters in the System Rhenium–Sulfur–Chlorine: Solid State Synthesis, Solution Chemistry, and Redox Properties

**Jean-Christophe Gabriel, Kamal Boubekeur,† and Patrick Batail*,†**

Laboratoire de Physique des Solides Associé au CNRS, Université de Paris-Sud, 91405 Orsay, France

*Received December 29, 1992*

Exploration of the Rb–Re–S–Cl system to identify soluble salts of molecular forms of octahedral $Re_6$ cluster anions has produced single crystals of $Rb[Re_6S_5Cl_9]$ (**1**) (monoclinic, space group $C2/c$, $a$ = 16.243(2) Å, $b$ = 9.252(4) Å, $c$ = 15.096(6) Å, $\beta$ = 113.37(3)°, and $Z$ = 4) and $(Rb^+)_5[Re_6S_6Cl_8^{2-}][Re_6S_7Cl_7^{3-}]$ (**2**) (cubic, space group $Pn\bar{3}$, $a$ = 13.342(4) Å, $Z$ = 4) as well as single crystals of the neutral linear-chain polymer $[Re_6S_5Cl_8]$ (**3**) (triclinic, space group $P\bar{1}$, $a$ = 9.050(3) Å, $b$ = 13.045(4) Å, $c$ = 8.767(4) Å, $\alpha$ = 96.08(4)°, $\beta$ = 116.08(3)°, $\gamma$ = 80.50 (3)°, $Z$ = 2) and of the molecular phase $[Re_6S_4Cl_{10}]$ (**4**) (triclinic, space group $P\bar{1}$, $a$ = 8.910(2) Å, $b$ = 12.441 (2) Å, $c$ = 8.842(1) Å, $\alpha$ = 95.79(1)°, $\beta$ = 97.61(1)°, $\gamma$ = 83.68(1)°, $Z$ = 2). The compound $Rb[Re_6S_5Cl_9]$is washed in water at room temperature and dissolved in ethanol, again at room temperature; addition of $(Bu_4N)Cl$ precipitates $(Bu_4N)[Re_6S_5Cl_3(Cl_6)]$ (**5**) (orthorhombic, space group $Pna2_1$, $a$ = 17.147(4) Å, $b$ = 9.792(3) Å, $c$ = 22.294(5) Å, $Z$ = 4). When $Rb[Re_6S_5Cl_9]$ is washed with hot water and dissolved in hot ethanol, $(Bu_4N)_2[Re_6S_6Cl_2(Cl_6)]$ (**6**) (monoclinic, space group $P2_1/n$, $a$ = 12.452(2) Å, $b$ = 11.836(3) Å, $c$ = 18.495(3) Å, $\beta$ = 90.35(2)°, $Z$ = 2), the thermodynamically most stable cluster form, is obtained instead. Addition of $(Bu_4N)Cl$ to the solution obtained by washing $Rb[Re_6S_5Cl_9]$ with cold water gives the new (24e) cluster $(Bu_4N)_3[Re_6S_7Cl(Cl_6)]$ (**7**) (monoclinic, space group $C2/m$, $a$ = 14.249(3) Å, $b$ = 20.208(4) Å, $c$ = 13.206(2) Å, $\beta$ = 90.79(2)°, $Z$ = 2), suggesting that small amounts of the yet unknown phase $Rb_3[Re_6S_7Cl_7]$ are formed along with **1** in the high-temperature synthesis, also in agreement with the extreme water solubility of **2**. $[Re_6S_5Cl_8]$ is highly soluble in DMF, and the neutral solvated cluster $[Re_6S_5Cl_8(DMF)]$ (**8**) has been prepared. Addition of $(Bu_4N)Cl$ to DMF solutions of $[Re_6S_5Cl_8]$ provide an alternative route to $(Bu_4N)[Re_6S_5Cl_9]$. Analysis of structural correlations in the unique series of crystal structures of $[Re_6S_4Cl_{10}]$ and $(Bu_4N)_n[Re_6S_{4+n}Cl_{10-n}]$, ($n$ = 1 (**5**), 2 (**6**), 3 (**7**)), determined by X-ray analysis, reveals a contraction of the cluster core upon addition of sulfur atoms. This contraction is not regular but is more pronounced between the $[Re_6S_5Cl_3]^{5+}$ and $[Re_6S_6Cl_2]^{4+}$ cluster cores. This discontinuity is also observed in the redox properties of the series of cluster anions, $[Re_6S_6Cl_8]^{2-}$ and $[Re_6S_7Cl_7]^{3-}$ being reversibly oxidized in acetonitrile (at ca. 1.0 V vs SCE) to the corresponding paramagnetic (23e) species.

## Introduction

The design of molecular hybrid salts of organic–inorganic character by electrochemical association of organic cation radicals with soluble, redox-active and photoactive molecular cluster or polynuclear anions such as $Mo_6Cl_{14}^{2-}$,[1] $Re_6Se_5Cl_9^-$,[2,3] $Mo_6Br_{14}^{2-}$,[4a,b] $Mo_6Cl_8(NCS)_6^{2-}$,[4c] $Nb_6Cl_{18}^{3-}$,[4d] and $SiW_{12}O_{40}^{4-}$,[4e] has provided the basis for a rich structural chemistry. The conducting, magnetic, or optical properties of such solids often critically depend on their type and degree of order, hence the need for high-quality single crystals. A prerequisite to such electrocrystallization experiments[5] is the solubility of the molecular precursors in a common, nonaqueous polar solvent, and indeed, the tetraalkylammonium salts of those all-inorganic cluster or polynuclear anions present the common property of being soluble in a variety of polar organic solvents.

Our primary incentive in selecting[2] $Re_6Se_5Cl_9^-$ was to extend our chemistry by electrochemically inducing such associations with a *monoanion*, isostructural and isoelectronic with $Mo_6Cl_{14}^{2-}$. To that effect, we sought molecular, discrete forms of such cluster anions among the wealth of fascinating new phases produced by Leduc, Perrin, and Sergent in their exploration of the Re–chalcogen (S, Se)–Cl system.[6] Indeed, these authors had shown that this chemistry is dominated by the presence of octahedral $Re_6$ cluster motifs (Figure 1) whose inner cores differ solely by the chalcogen/halogen ratio of the eight atoms capping the faces of the $Re_6$ octahedron. A variety of linkages between the cluster motifs (by sharing some or all of the six outer chloride ligands), associated with different charge states of the cluster, has been identified.[6] The synthesis of novel salts where cluster anions exist in a molecular form, that is, whose cluster cores are surrounded by terminal chloride ($Cl_t$) only (as shown in Figure 1), became of particular interest[7] after our initial observation

† Work initiated when these authors were at the Laboratoire de Chimie Inorganique et Moléculaire, URA CNRS 254, Université de Rennes I, France.

(1) Ouahab, L.; Batail, P.; Perrin, C.; Garrigou-Lagrange, C. *Mater. Res. Bull.* **1986**, *21*, 1223.

(2) Batail, P.; Ouahab, L.; Pénicaud, A.; Lenoir, C.; Perrin, A. *C. R. Acad. Sci., Ser. 2* **1987**, *304*, 1111.

(3) (a) Renault, A.; Pouget, J.-P.; Parkin, S. S. P.; Torrance, J. B.; Ouahab, L.; Batail, P. *Mol. Cryst. Liq. Cryst. Inc. Nonlin. Opt.* **1988**, *161*, 329. (b) Pénicaud, A.; Lenoir, C.; Batail, P.; Coulon, C.; Perrin, A. *Synth. Met.* **1989**, *32*, 25. (c) Pénicaud, A.; Boubekeur, K.; Batail, P.; Canadell, E.; Auban-Senzier, P.; Jérome, D. *J. Am. Chem. Soc.*, in press.

(4) (a) Batail, P.; Livage, C.; Parkin, S. S. P.; Coulon, C.; Martin, J. D.; Canadell, E. *Angew. Chem., Int. Ed. Engl.* **1991**, *30*, 1498. (b) Jarchow, S.; Fourmigué, M.; Batail, P. *Acta Crystallogr., Sect. C*, in press. (c) Guirauden, A.; Johannsen, I.; Batail, P.; Coulon, C. *Inorg. Chem.*, in press. (d) Pénicaud, A.; Batail, P.; Davidson, P.; Levelut, A.-M.; Coulon, C.; Perrin, C. *Chem. Mater.* **1990**, *2*, 117. (e) Davidson, A.; Boubekeur, K.; Pénicaud, A.; Auban, P.; Lenoir, C.; Batail, P.; Hervé, G. *J. Chem. Soc., Chem. Commun.* **1989**, 1373.

(5) The electrocrystallization technique has emerged in the last decade as a powerful and versatile tool to provoke the association of a large variety of molecular ions into high-purity single crystals. See, for example: (a) Chiang, T. C.; Reddoch, A. H.; Williams, D. F. *J. Chem. Phys.* **1971**, *54*, 2051. (b) Kathirgamanathan, P.; Mucklejohn, S. A.; Rosseinsky, D. R. *J. Chem. Soc., Chem. Commun.* **1979**, 86. (c) Bechgaard, K.; Carneiro, K.; Rasmussen, F. B.; Olsen, M.; Rindorf, G.; Jacobsen, C. S.; Pedersen, H. J.; Scott, J. C. *J. Am. Chem. Soc.* **1981**, *103*, 2440. (d) Enkelmann, V.; Morra, B. S.; Wegner, G.; Heinze, J. *Chem. Phys.* **1982**, *66*, 303. (e) Ward, M. D. *J. Electroanal. Chem. Interfacial Electrochem.* **1989**, *273*, 79. (f) Echegoyen, L.; De Cian, A.; Fischer, J.; Lehn, J.-M. *Angew. Chem., Int. Ed. Engl.* **1991**, *30*, 838. (g) Williams, J. M.; Ferraro, J. R.; Thorn, R. J.; Carlson, K. D.; Geiser, U.; Wang, H. H.; Kini, A. M.; Whangbo, M.-H. In *Organic Superconductors*; Prentice Hall: Englewood Cliffs, NJ, 1992, pp 43–45.

(6) Leduc, L.; Perrin, A.; Sergent, M. *C. R. Acad. Sci., Ser. 2* **1983**, *296*, 961.

0020-1669/93/1332-2894$04.00/0 

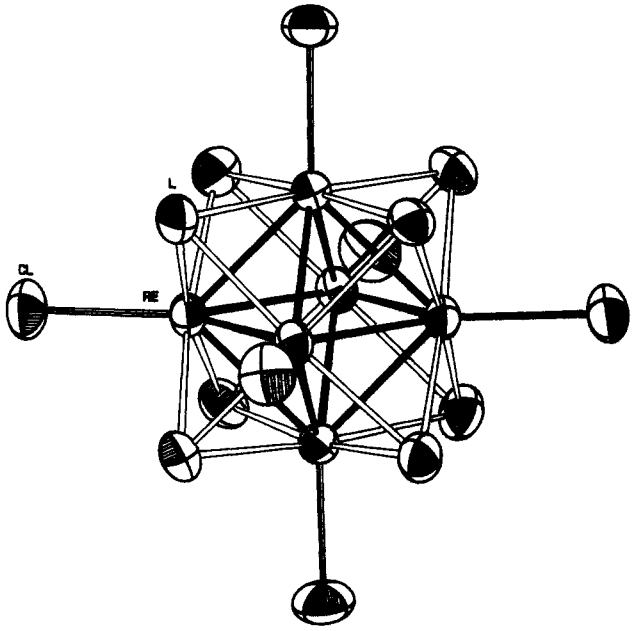


**Figure 1.** Ortep representation of the structure of $[Re_6S_6Cl_8]^{2-}$ in **6**. This structure is common to **1**–**7**. The thermal ellipsoids are drawn at the 50% probability level. The face-capping ligands L are composite S/Cl atoms, weighted accordingly, as described in the Experimental Section. The cluster molecule is totally asymmetric in **5**; it is centrosymmetric (site symmetry $\bar{1}$) in **1**, **3**, **4**, and **6**; its site symmetry is $2/m$ for **7** and $\bar{3}$ for **2**.

that the potassium salt of $[Re_6Se_5Cl_3(Cl_t)_6]^-$ is soluble in ethanol where metathesis with tetraalkylammonium cations occurs readily to give, for example, $(Bu_4N)[Re_6Se_5Cl_9]$.[2]

In this paper we report our work with sulfido–chlorine $Re_6$ clusters, beginning with the observation that $Rb[Re_6S_5Cl_9]$ is also found to be soluble in ethanol and acetone, followed by the subsequent synthesis of $(Bu_4N)[Re_6S_5Cl_9]$. Then, having obtained $[Re_6S_6Cl_8]^{2-}$ by thermal treatment in solution[8] and the cluster $[Re_6S_7Cl_7]^{3-}$ described in this paper, we search the largely unexplored Rb–Re–S–Cl system for their corresponding alkali metal salts. The solid-state synthesis reported here was designed to prepare the series of salts $Rb_n[Re_6S_{4+n}Cl_{10-n}]$, ($n$ = 1–3) of an alkali metal cation and provide an entry into the solution-phase chemistry of these molecular cluster forms[9,10] with a variety of negative charges.

## Experimental Section

**High-Temperature Synthesis.** All reactants were purchased from commercial sources. The following general procedure applies for each compound. In the inert argon atmosphere of a drybox, Re powder, $ReCl_5$, S, and anhydrous RbCl are mixed in the appropriate proportions and pressed into a pellet which is introduced in a silica tube (inner diameter 7 mm; external diameter 9 mm; ca. 45 mm long, when sealed) closed with a valve. The bottom part of this tube is cooled in liquid nitrogen to prevent any sublimation of $ReCl_5$, evacuated to ca. $10^{-5}$ Torr of residual pure argon, sealed, and placed in a vertical furnace.

**(a) $Rb[Re_6S_5Cl_9]$ (1).** The pellet is prepared by mixing Re (292 mg, 1.57 mmol), $ReCl_5$ (207 mg, 0.57 mmol), S (55 mg, 1.72 mmol), and RbCl (43 mg, 0.36 mmol). The furnace temperature is raised at a rate of 1 °C $min^{-1}$ up to 850 °C where it is maintained for 24 h. Cooling down to room temperature is achieved at a rate of 6 °C $min^{-1}$. Finally, the furnace is brought back slightly off the horizontal and the silica tube is shifted over at the upper end of the furnace where it is allowed to stand for 1 h in a temperature gradient (300–25 °C). The purpose of this final treatment is to ensure that all remaining volatile products will condense away at the upper end of the tube. A dark red-brown crystalline powder is obtained that way. High-quality, dark red single crystals are grown with the following slightly different thermal treatment: the high-temperature plateau is now fixed at 820 °C and kept for 8 h followed by a slow cooling down to 150 °C at 1 °C $h^{-1}$, then down to 100 °C at 2 °C $h^{-1}$, and, finally, down to room temperature at 1 °C $min^{-1}$. The furnace is rotated back to horizontal when the temperature reaches 150 °C. Note that similar runs were performed using larger, 10.5 mm × 13.5 mm × 100 mm silica tubes containing a pellet composed of Re (1.116 g, 6 mmol), $ReCl_5$ (0.792 g, 2.18 mmol), S (0.209 g, 6.52 mmol), and RbCl (0.164 g, 1.36 mmol).

**(b) $Rb_{2.5}[Re_6S_{6.5}Cl_{7.5}]$ (2).** The pellet is prepared by mixing Re (338 mg, 1.82 mmol), $ReCl_5$ (330 mg, 0.91 mmol), S (95 mg, 2.96 mmol), and RbCl (200 mg, 1.65 mmol). Orange single crystals are obtained by slowly heating the tube (1 °C $h^{-1}$) up to 825 °C, where it is kept for 1 h before cooling down to room temperature at 5 °C $h^{-1}$.

**(c) $[Re_6S_5Cl_8]$ (3).** The pellet is prepared by mixing Re (186 mg, 1.00 mmol), $ReCl_5$ (132 mg, 0.36 mmol), and S (29 mg, 0.90 mmol). High-quality dark red single crystals, easily cleaved into elongated needles, are obtained by heating the tube at the rate of 1 °C $min^{-1}$ up to 450 °C, then at 0.5 °C $min^{-1}$ up to 825 °C, where it is kept for 100 h before cooling at 1 °C $h^{-1}$ down to 600 °C, then at 2 °C $h^{-1}$ down to 250 °C, and at 1 °C $h^{-1}$ to reach room temperature. Larger quantities of the compound are obtained using the larger silica tube with the following amounts and conditions: Re (893 mg, 4.80 mmol), $ReCl_5$ (634 mg, 1.74 mmol), and S (139 mg, 4.34 mmol); up to 450 °C at 1 °C $min^{-1}$ and then at 0.5 °C $min^{-1}$ up to 825 °C, where it is kept 11 days before cooling down to room temperature at 1 °C $min^{-1}$. Note that ca. 800 mg out of a total of 1.2 g of solid product is in fact obtained as large single crystals in the outer (colder) end of the silica tube.

**(d) $[Re_6S_4Cl_{10}]$ (4).** A pellet, prepared by mixing Re (338 mg, 1.82 mmol), $ReCl_5$ (330 mg, 0.91 mmol), and S (58 mg, 1.81 mmol), is subjected to a thermal treatment identical to that given for $Re_6S_5Cl_8$ and found to yield a mixture of dark red single crystals of $Re_6S_4Cl_{10}$ together with crystals of $Re_6S_5Cl_8$. The latter are identified by their cleaving ability and unit cell. This compound is identified by a single-crystal X-ray structure determination.

**Solution-Phase Chemistry. (a) $[Re_6S_5Cl_8(DMF)]$·2.5DMF (8).** $Re_6S_5Cl_8$ (200 mg, 0.13 mmol) is stirred at 30 °C for 12 h in dimethylformamide (20 mL). The red DMF solution is filtered off, the solvent is removed under vacuum, and the residue is vacuum-dried at 80 °C for 48 h to yield 191 mg of an orange crystalline powder. Anal. Calcd for $C_{10.5}H_{24.5}N_{3.5}O_{3.5}Re_6S_5Cl_8$: C, 6.94; H, 1.36; N, 2.70; S, 8.82; Cl, 15.61. Found: C, 7.43; H, 1.39; N, 2.58; S, 8.40; Cl, 15.65. Recrystallization in DMF yields pale yellow, platelike single crystals. The compound crystallizes in a monoclinic unit cell, space group $C2/c$, with, at 170 K, $a$ = 18.25(2) Å, $b$ = 10.507(5) Å, $c$ = 20.13(1) Å, $\beta$ = 107.67(7)°, $V$ = 3678 Å$^3$, and $Z$ = 8. The crystals are poor X-ray scatterers, indicating a fair amount of structural disorder.

**(b) $(Bu_4N)[Re_6S_5Cl_9]$ (5).** A few pellets of crude $RbRe_6S_5Cl_9$ (2.283 g) are ground and stirred for 3 h *at room temperature* in water (1 L); the mixture is then acidified with a few drops of concentrated hydrochloric acid, to yield a dark brown suspension which is filtered to isolate a brown solid residue (1.602 g). The resulting pale yellow solution is treated separately (see, below, the preparation of $(Bu_4N)_3Re_6S_7Cl_7$). The brown precipitate is dried in vacuo and dissolved upon stirring in absolute ethanol (2 l) for 24 h. The orange-yellow ethanolic solution is filtered off to remove an insoluble dark gray residue consisting of metallic rhenium (0.354 g). The solution is concentrated without external heating prior to the addition of an ethanolic solution of tetrabutylammonium chloride. The mixture is left to stand for a few hours upon which an orange microcrystalline precipitate appears. The crystalline powder material is collected on a glass frit, washed with ethanol, and dried in vacuo. The compound is recrystallized from acetonitrile to give 1.635 g ( 63%) of red-orange parallelepipedic crystals. Anal. Calcd for $C_{16}H_{36}NRe_6S_5Cl_9$: C, 10.45; H, 1.97; N, 0.76; Cl, 17.34; S, 8.71. Found: C, 10.45; H, 1.91; N, 0.91; Cl, 17.25; S, 8.45.

**(c) $(Bu_4N)_2[Re_6S_6Cl_8]$ (6).** The above procedure applies to the preparation of this compound with the difference that the initial water treatment occurs at 70 °C and the dissolution in ethanol at 50 °C. The addition of tetrabutylammonium chloride to the ethanolic solution gives

(7) As exemplified by recent similar work by Holm and co-workers in the search for such molecular forms in the Re–Se–Cl system and their subsequent solution-phase chemistry, which appeared when we had completed the preparation of this manuscript: Yaghi, O. M.; Scott, M. J.; Holm, R. H. *Inorg. Chem.* **1992**, *31*, 4778. See also: Lee, S. C.; Holm, R. H. *Angew. Chem., Int. Ed. Engl.* **1990**, *29*, 840.

(8) Boubekeur, K. Thesis, Université de Rennes I, 1989.

(9) Gabriel, J.-C.; Johannsen, I.; Batail, P.; Coulon, C. *Acta Crystallogr.*, in press.

(10) Coulon, C.; Livage, C.; Gonzalvez, L.; Boubekeur, K.; Batail, P. *J. Phys. I*, in press.

a red-orange precipitate which yields beautiful ruby red octahedra upon recrystallization in acetonitrile. This compound is identified by a single-crystal X-ray structure determination.

**(d) $(Bu_4N)_3[Re_6S_7Cl_7]$ (7).** The yellow aqueous solution resulting from the *room temperature* acid treatment of $Rb[Re_6S_5Cl_9]$ is concentrated and filtered to remove a yellow-green residue of $Rb_2ReCl_6$ (13 mg). An ethanolic solution of tetrabutylammonium chloride is then added, and an orange precipitate forms rapidly. The latter microcrystalline powder is filtered off, dried in vacuo, and found to be highly soluble in acetonitrile. It is recrystallized from methanol–acetonitrile solutions to yield 0.618 g (19%) of red-orange, plate-shaped single crystals. Anal. Calcd for $C_{48}H_{108}N_3Re_6S_7Cl_7$: C, 24.88; H, 4.66; N, 1.81. Found: C, 24.67; H, 4.71; N, 1.83.

**X-ray Crystallography.** Experimental details for compounds **1–7** are given in Table I. In each case, a suitable single crystal was mounted on a glass fiber in a random orientation. Preliminary examination and data collection were performed on a $\kappa$-axis Enraf-Nonius CAD4-F diffractometer using graphite monochromatized Mo K$\alpha$ radiation. The unit cell dimensions and crystal orientation matrix were derived from least-squares refinement of setting angles of 25 reflections. Intensity data were collected using the $\omega$–$2\theta$ scan mode (or pure $\omega$ scan mode for $Re_6S_4Cl_{10}$) with the following conditions: $\omega$ scan width $\Delta\omega = (a + 0.35 \tan\theta)°$ extended 25% on each side for background measurement, horizontal aperture $(b + 0.5 \tan\theta)$ mm, vertical aperture 4 mm, prescan speed 10° min$^{-1}$, $\sigma(I)/I = 0.01$, maximum time for final scan 60 s. The orientation was checked every 400 reflections and maintained within 0.10°. As a check on crystal and electronic stability, three representative reflections were measured every hour of X-ray exposure time. Data were corrected for background, Lorentz, polarization, and absorption effects. Absorption corrections were applied using empirical procedures based either on azimuthal $\psi$ scans of some reflections having a Eulerian angle $\chi$ near 90° ($\kappa > 100°$)[11] or on the DIFABS algorithm.[12] The structures were solved by direct methods using MULTAN11/82[13] or by the Patterson method and refined (on F's) by full-matrix least-squares calculations initially with isotropic and finally with anisotropic thermal parameters for non-H atoms (except when stated). The atomic scattering factors and anomalous dispersion corrections were from ref 14. All calculations were performed on a microVAXII computer by using the Enraf-Nonius SDP/PLUS system of programs.[15] The similarity of the X-ray scattering power of sulfur and chlorine atoms makes it difficult to ascertain whether these atoms are localized or disordered over all crystallographically independent, face-capping sites. It was thus assumed that these sites are shared by S and Cl atoms with a statistical occupancy, and in the last refinement cycles these positions were refined with an appropriately averaged scattering factor. In addition, the tetrabutylammonium cations were found to be severely affected by large thermal motion and/or disorder. In general, the difference Fourier maps failed to suggest a suitable disorder model for several of their carbon atoms. Many parameters are necessary to model reasonably the electron density in these areas of the unit cell. It was outside the scope of this work to optimize further the geometry of the tetrabutylammonium cations, and even if the reliability factors may be somewhat high, the connectivity and bond lengths and angles of all $[Re_6S_{4+n}Cl_{10-n}]^{n-}$ ($n$ = 1–3) anions are well defined.

**Structure Solution. (a) $Rb[Re_6S_5Cl_9]$.** A parallelepipedic dark red crystal with dimensions 0.15 × 0.15 × 0.09 mm$^3$ was used. A total of 5856 intensities were recorded ($\theta \le 28°$) at room temperature in the quadrants $+h,\pm k,\pm l$. An empirical absorption correction based on the DIFABS procedure was applied (correction coefficients ranged from 0.76 to 1.38) to the reflection data. Data reduction and averaging yielded 2768 independent reflections ($R_{int}$ = 0.041), of which 1884, with $I \ge 3\sigma(I)$, were used for the calculations. Systematic extinctions were consistent with either the noncentrosymmetric $Cc$ or the centrosymmetric $C2/c$ space group. The latter was chosen from intensity statistics and confirmed by success of structure refinements. The structure was solved by direct methods, which revealed three independent rhenium atoms in general positions. The remaining atoms were found on successive difference Fourier maps. All atoms were refined anisotropically. The asymmetric unit consists of one-half of a cluster anion and one rubidium on a special position. The cluster core face-capping atoms were considered disordered, and their positions were refined with site occupancies of $^3/_8$ Cl + $^5/_8$ S.

**(b) $Rb_{2.5}[Re_6S_{6.5}Cl_{7.5}]$.** A prismatic red-orange crystal with dimensions 0.06 × 0.06 × 0.06 mm$^3$ was used. A total of 6220 intensities were recorded ($\theta \le 28°$) at room temperature in the quadrants $+h,\pm k,+l$. An empirical absorption correction based on the DIFABS procedure was applied (correction coefficients ranged from 0.73 to 1.44) to the reflection data. Data reduction and averaging yielded 967 independent reflections ($R_{int}$ = 0.073) of which 213 had $I \ge 2\sigma(I)$ and were used for the calculations. Systematic extinctions were consistent with either the $Pn\bar{3}$ or the $Pn\bar{3}m$ space group. The former was chosen after checking the Laue class and confirmed by success of structure refinements. The structure was solved by direct methods, which revealed one independent rhenium atom in a general position. The remaining atoms were found on successive difference Fourier maps. All atoms were refined anisotropically. The asymmetric unit consists of one rhenium, one chlorine, two mixed ligands, and two rubidium atoms. The cluster core face-capping atoms were considered disordered, and their positions were refined with site occupancies of $^3/_{16}$ Cl + $^{13}/_{16}$ S.

**(c) $[Re_6S_5Cl_8]$.** A tabular red crystal with dimensions 0.03 × 0.06 × 0.05 mm$^3$ was used. A total of 4694 intensities were recorded ($\theta \le 28°$) at room temperature in the quadrants $+h,\pm k,\pm l$. An empirical absorption correction based on the DIFABS procedure was applied (correction coefficients ranged from 0.88 to 1.07) to the reflection data. Data reduction and averaging yielded 2768 independent reflections ($R_{int}$ = 0.026), of which 2685 had $I \ge 3\sigma(I)$ and were used for the calculations. Systematic extinctions were consistent with either the noncentrosymmetric $P1$ or the centrosymmetric $P\bar{1}$ space group. The latter was chosen from intensity statistics and confirmed by success of structure refinements. The structure was solved by direct methods, which revealed six independent rhenium atoms in general positions. The remaining atoms were found on successive difference Fourier maps. All atoms were refined anisotropically. The asymmetric unit consists of two half-cluster anions. The cluster core face-capping atoms were considered disordered, and their positions were refined with site occupancies of $^3/_8$ Cl + $^5/_8$ S.

**(d) $[Re_6S_4Cl_{10}]$.** An plate-shaped red crystal with dimensions 0.03 × 0.12 × 0.21 mm$^3$ was used. A total of 4842 intensities were recorded ($\theta \le 28°$) at room temperature in the quadrants $\pm h,\pm k,+l$. An empirical absorption correction based on the DIFABS procedure was applied (correction coefficients ranged from 0.78 to 1.57) to the reflection data. Data reduction and averaging yielded 4629 independent reflections ($R_{int}$ = 0.015) of which 3506 had $I \ge 3\sigma(I)$ and were used for the calculations. Systematic extinctions were consistent with either the noncentrosymmetric $P1$ or the centrosymmetric $P\bar{1}$ space group. The latter was chosen from intensity statistics and confirmed by success of structure refinements. The structure was solved by direct methods, which revealed six independent rhenium atoms in general positions. The remaining atoms were found on successive difference Fourier maps. All atoms were refined anisotropically. The asymmetric unit consists of two half-cluster anions. The cluster core face-capping atoms were considered disordered, and their positions were refined with site occupancies of $^1/_2$ Cl + $^1/_2$ S.

**(e) $(Bu_4N)[Re_6S_5Cl_9]$.** A parallelepipedic red-orange crystal with dimensions 0.27 × 0.14 × 0.13 mm$^3$ was used. A total of 8247 intensities were recorded ($\theta \le 26°$) at room temperature in the quadrants $\pm h,\pm k,+l$. An empirical absorption correction based on eight $\psi$-scanned reflections around the diffraction vector (transmission factors ranged from 0.73 to 0.99) was applied to the reflection data. Data reduction and averaging now yielded 3197 independent reflections ($R_{int}$ = 0.037), of which 1522 had $I \ge 3\sigma(I)$ and were used for the calculations. Systematic extinctions were consistent with either the centrosymmetric $Pnma$ or the noncentrosymmetric $Pna2_1$ space group. The latter was chosen from intensity statistics and confirmed by success of structure refinements. The structure was solved by direct methods, which revealed six independent rhenium atoms in general positions. The remaining atoms were found on successive difference Fourier maps. All atoms of the cluster anion were refined anisotropically whereas the atoms of the cations were refined isotropically. The asymmetric unit consists of one cluster anion and one cation. The cluster core face-capping atoms were considered disordered, and their positions were refined with site occupancies of $^3/_8$ Cl + $^5/_8$ S.

**(f) $(Bu_4N)_2[Re_6S_6Cl_8]$.** An octahedron-shaped red crystal with dimensions 0.09 × 0.09 × 0.09 mm$^3$ was used. A total of 11455 intensities

(11) North, A. C. T.; Philips, D. C.; Matthews, F. S. *Acta Crystallogr.* **1968**, *A24*, 351.
(12) Walker, D.; Stuart, N. *Acta Crystallogr.* **1983**, *A39*,158.
(13) Main, P.; Fiske, S. J.; Hull, S. E.; Lessinger, L.; Germain, G.; Declercq, J.-P.; Woolfson, M. M. MULTAN11/82: A System of Computer Programs for the Automatic Solution of Crystal Structures from X-ray Diffraction Data. Universities of York, England, and Louvain, Belgium, 1982.
(14) *International Tables for X-Ray Crystallography*; Kynoch Press: Birmingham, U.K., 1974; Vol. IV.
(15) Frenz, B. A. *Enraf-Nonius SDP-Plus Structure Determination Package*, Version 3.0; Enraf-Nonius: Delft, The Netherlands, 1985.

**Table I.** Crystallographic Data for $Rb[Re_6S_5Cl_9]$ (**1**), $Rb_{2.5}[Re_6S_{6.5}Cl_{7.5}]$ (**2**), $[Re_6S_5Cl_8]$ (**3**), $[Re_6S_4Cl_{10}]$ (**4**), $(Bu_4N)[Re_6S_5Cl_9]$ (**5**), $(Bu_4N)_2[Re_6S_6Cl_8]$ (**6**), and $(Bu_4N)_3[Re_6S_7Cl_7]$ (**7**)

| | **1** | **2** | **3** | **4** | **5** | **6** | **7** |
|---|---|---|---|---|---|---|---|
| formula | $Cl_9RbRe_6S_5$ | $Cl_{7.5}Rb_{2.5}Re_6S_{6.5}$ | $Cl_8Re_6S_5$ | $Cl_{10}Re_6S_4$ | $C_{16}H_{36}Cl_9NRe_6S_5$ | $C_{32}H_{72}Cl_8N_2Re_6S_6$ | $C_{48}H_{108}Cl_7N_3Re_6S_7$ |
| fw | 1682.07 | 1805.19 | 1561.14 | 1599.99 | 1835.04 | 2078.15 | 2317.24 |
| cryst syst | monoclinic | cubic | triclinic | triclinic | orthorhombic | monoclinic | monoclinic |
| space group | $C2/c$ | $Pn\bar{3}$ | $P\bar{1}$ | $P\bar{1}$ | $Pna2_1$ | $P2_1/n$ | $C2/m$ |
| $a$, Å | 16.243(2) | 13.342(4) | 9.050(3) | 8.910(2) | 17.147(4) | 12.452(2) | 14.249(3) |
| $b$, Å | 9.252(4) | | 13.045(4) | 12.441(2) | 9.792(3) | 11.836(3) | 20.208(4) |
| $c$, Å | 15.096(6) | | 8.767(4) | 8.842(1) | 22.294(5) | 18.495(3) | 13.206(2) |
| $\alpha$, deg | | | 96.08(4) | 95.79(1) | | | |
| $\beta$, deg | 113.37(3) | | 116.08(3) | 97.61(1) | | 90.35(2) | 90.79(2) |
| $\gamma$, deg | | | 80.50(3) | 83.68(1) | | | |
| $V$, Å$^3$ | 2082.5(7) | 2375.0(2) | 916.0(15) | 962.0(5) | 3743.2(2.9) | 2725.9(1.6) | 3802.2(2.1) |
| $Z$ | 4 | 4 | 2 | 2 | 4 | 2 | 2 |
| $d$(calc), g·cm$^{-3}$ | 5.36 | 5.05 | 5.66 | 5.52 | 3.26 | 2.53 | 2.02 |
| $\mu$, cm$^{-1}$ | 391.2 | 372.4 | 417.4 | 399.3 | 205.3 | 140.9 | 101.1 |
| $R^a$ | 0.036 | 0.023 | 0.031 | 0.034 | 0.031 | 0.045 | 0.070 |
| $R_w{}^b$ | 0.041 | 0.022 | 0.036 | 0.051 | 0.041 | 0.053 | 0.087 |
| goodness of fit $S^c$ | 1.023 | 0.505 | 1.027 | 1.764 | 1.155 | 1.363 | 2.052 |

$^a$ $R = \sum||F_o|-|F_c||/\sum|F_o|$. $^b$ $R_w = [\sum w(|F_o|-|F_c|)^2/\sum w|F_o|^2]^{1/2}$; $\omega = [\sigma^2(I) + (pF_o^2)^2]^{-1}$. $^c$ $S = [\sum w(F_o^2-F_c^2)^2/(n-v)]^{1/2}$.

were recorded ($\theta \le 27°$) at room temperature in the quadrants $\pm h,\pm k,+l$. A slight decay of 4% was observed during the 119 h of X-ray exposure time, and the data were corrected accordingly. An empirical absorption correction (volume absorption coefficient $\mu = 140.9$ cm$^{-1}$) based on seven $\psi$-scanned reflections around their diffraction vector (transmission factors ranged from 0.56 to 0.99) was applied to the reflection data. Data reduction and averaging yielded 5543 independent reflections ($R_{int}$ = 0.013) of which 2102 had $I \ge 3\sigma(I)$ and were used for the calculations. Systematic extinctions were consistent with the unambiguous centrosymmetric $P2_1/n$ space group (nonconventionnal setting of $P2_1/c$). The structure was solved by the Patterson method, which revealed three independent rhenium atoms in general positions. The remaining atoms were found on successive difference Fourier maps. In the final least-squares refinement, the atoms of the anion cluster were refined anisotropically and the atoms of the tetrabutylammonium cation were refined isotropically. The cluster core face-capping atoms were considered disordered, and their positions were refined with site occupancies of $^2/_8$ Cl + $^6/_8$ S. The final difference Fourier map contained a series of peaks in the vicinity of the rhenium atoms. Due to the high thermal motion of the carbon atoms of the cation, hydrogen atoms could not be located and therefore were not considered. The asymmetric unit consists of one-half of a cluster anion and one cation.

**(g) $(Bu_4N)_3[Re_6S_7Cl_7]$.** A plate-shaped red-orange crystal with dimensions 0.30 × 0.15 × 0.03 mm$^3$ was used. A total of 7818 intensities were recorded ($\theta \le 26°$) at room temperature in the quadrants $+h,\pm k,\pm l$. The standard reflections showed no decay in the intensity (0.5% over the 79.8 h of X-ray exposure time). An empirical absorption correction (correction factors ranged from 0.45 to 1.42) was applied to the reflection data. Data reduction and averaging now yielded 3843 independent reflections ($R_{int}$ = 0.049), of which 1474 had $I \ge 3\sigma(I)$ and were used for the calculations. Systematic extinctions were consistent with either the noncentrosymmetric space groups $C2$ and $Cm$ or the centrosymmetric one $C2/m$. The structure was solved in the last space group by direct methods, which revealed two independent rhenium atoms (one atom in general position and one atom on the mirror plane). The remaining atoms were located by a series of least-squares refinements and successive difference Fourier syntheses. In the final least-squares refinement, the atoms of the anion cluster were refined anisotropically and the atoms of the tetrabutylammonium cations were refined isotropically. The cluster core face-capping atoms were considered disordered, and their positions were refined with site occupancies of $^1/_8$ Cl + $^7/_8$ S. In addition to the large thermal motion of the carbon atoms, one tetrabutylammonium cation was found to be very highly disordered. With a nitrogen atom located on a site symmetry $2/m$, an alkyl chain was found in general position and a second one was located on the mirror plane. The final difference Fourier map contained a series of peaks located on and near the mirror plane. Every attempt to model them as the missing alkyl chain failed. In view of the severe disorder and high thermal motion of the cations, no attempt was made to locate or introduce the hydrogen atoms. The asymmetric unit consists of one-quarter of a cluster anion and three-quarters of a cation.

Final $R$ factors for compounds **1**–**7** are given in Table I. Other crystallographic data are available as supplementary material.

**Electrochemistry.** Cyclic voltammograms were obtained by using a PAR 273 potentiostat with a platinum-disk working electrode (o.d. = 1 mm), a platinum-wire counter electrode, and a Taccussel SCE reference electrode. The ferrocene/ferrocenium couple was used as an internal standard.

## Results and Discussion

**Solid-State Synthesis of Re–S–Cl Molecular Entities.** At the onset of this study, the only anions in molecular form known in the Re–chalcogen–Cl system and characterized by a full single-crystal structure determination were those of $K[Re_6Se_5Cl_9]$[16] and $Pb[Re_6Se_6Cl_8]$.[17] In addition, a few such salts had been reported and characterized solely by their X-ray powder patterns by analogy with the former two structures. These include $M^I[Re_6Se_5Cl_9]$ ($M^I$ = Li, Na, Rb, Cu, Ag)[16] and $Cd[Re_6Se_6Cl_8]$[17] as well as $M^I[Re_6S_5Cl_9]$ ($M^I$ = Ag, Rb).[16]

Thus, the previously described[16] synthesis of $Rb[Re_6S_5Cl_9]$ was scaled up in order to prepare larger quantities and obtain good X-ray-quality single crystals. The latter were found to be soluble in ethanol and acetone. Addition of $(Bu_4N)Cl$ to the former ethanol solution precipitates $(Bu_4N)[Re_6S_5Cl_9]$. The solid-state synthesis reported here was designed to prepare a series of salts, $Rb_n[Re_6S_{4+n}Cl_{10-n}]$ ($n$ = 1–3), of an alkali metal cation. The novel phase $Rb_{2.5}[Re_6S_{6.5}Cl_{7.5}]$ was then obtained, and its crystal structure revealed the coexistence of both $[Re_6S_6Cl_8]^{2-}$ and $[Re_6S_7Cl_7]^{3-}$ cluster forms within a single composite salt, $(Rb^+)_5[Re_6S_6Cl_8^{2-}][Re_6S_7Cl_7^{3-}]$. This demonstrates that the solid-state synthesis of $[Re_6S_7Cl_7]^{3-}$ has indeed been achieved here for the first time. This also suggests that selective synthesis of the yet unknown salts $Rb_2[Re_6S_6Cl_8]$ and $Rb_3[Re_6S_7Cl_7]$ should be possible. In addition, two novel phases, $[Re_6S_4Cl_{10}]$ and $[Re_6S_5Cl_8]$, were obtained. The former contains the neutral cluster molecule $[(Re_6S_4Cl_4)(Cl_t)_6]$, with all six outer, terminal chlorine atoms ($Cl_t$) unshared in the solid state. In the latter, two outer, bridging terminal chlorine atoms ($Cl_b$) are shared to form the linear-chain inorganic polymer $[(Re_6S_5Cl_3)(Cl_t)_4(Cl_b)_{2/2}]$.

**Core Substitution Achieved by Thermal Treatment in Solution.** Metathesis of $Rb[Re_6S_5Cl_9]$ with tetraalkylammonium cations occurs readily in dry ethanol to give, for example, $(Bu_4N)[Re_6S_5Cl_9]$. The initial washing in water was conducted to remove any small amount of $Rb_2ReCl_6$ which might be formed during the high-temperature synthesis. It then became apparent that, when the initial washing in water and subsequent dissolution in alcohol were conducted in hot solutions, typically 50–70 °C,

(16) Perrin, A.; Leduc, L.; Potel, M.; Sergent, M. *Mater. Res. Bull.* **1990**, *25*, 1227.
(17) Leduc, L. Thesis, Université de Rennes I, 1983.

**Table II.** Ranges and Mean Values of Interatomic Distances (Å) in the Neutral Cluster Molecule $Re_6S_4Cl_{10}$ and the Series of Ammonium Salts $(Bu_4N^+)_n[Re_6S_{4+n}Cl_{10-n}]^{n-}$ ($n$ = 1–3)

| | | $[(Re_6S_4Cl_4)Cl_6]$ | $[(Re_6S_5Cl_3)Cl_6]^-$ | $[(Re_6S_6Cl_2)Cl_6]^{2-}$ | $[(Re_6S_7Cl)Cl_6]^{3-}$ |
|---|---|---|---|---|---|
| Re–Re | mean | 2.595(2) | 2.589(7) | 2.573(8) | 2.570(10) |
| | range | 2.592(1)–2.599(1) | 2.576(2)–2.607(2) | 2.562(1)–2.583(1) | 2.560(1)–2.581(1) |
| Re–L | mean | 2.422(12) | 2.418(45) | 2.401(9) | 2.395(19) |
| | range | 2.401(3)–2.447(3) | 2.315(12)–2.513(13) | 2.384(5)–2.413(7) | 2.359(12)–2.422(7) |
| Re–$Cl_t$ | mean | 2.319(11) | 2.344(45) | 2.362(12) | 2.397(3) |
| | range | 3.201(6)–2.330(4) | 2.288(12)–2.396(12) | 2.353(7)–2.375(4) | 2.396(10)–2.401(5) |
| $(Re\cdots Re)_{trans}$ | mean | 3.669(2) | 3.662(5) | 3.639(12) | 3.636(3) |
| | range | 3.668(1)–3.673(1) | 3.657(2)–3.668(2) | 3.632(1)–3.653(1) | 3.633(1)–3.638(3) |

the metathesis yielded $(Bu_4N)_2[Re_6S_6Cl_8]$ instead.[8] This suggests that core reactions occur upon thermal treatment in solution to give $[Re_6S_6Cl_8]^{2-}$, which thus appears to be thermodynamically more stable than $[Re_6S_5Cl_9]^-$. Also unexpected was the precipitation of $(Bu_4N)_3[Re_6S_7Cl_7]$ by addition of $(Bu_4N)Cl$ to the water solution, albeit solely when solid $Rb[Re_6S_5Cl_9]$ was washed at room temperature. This tends to indicate that, besides $Rb[Re_6S_5Cl_9]$, small amounts of the unkown phase $Rb_3[Re_6S_7Cl_7]$ are formed in the high-temperature synthesis and that the latter is soluble in water. This was confirmed by the synthesis of $Rb_{2.5}[Re_6S_{6.5}Cl_{7.5}]$ (**2**) and the observation that **2** is extremely soluble in water.[18]

When solid $RbRe_6S_5Cl_9$ is processed in hot solutions, either one of the following reactions may occur. The first one is the conproportionation reaction

$$Re_6S_5Cl_9^- + Re_6S_7Cl_7^{3-} \rightarrow 2Re_6S_6Cl_8^{2-}$$

Equally probable, is the disproportionation reaction

$$2Re_6S_5Cl_9^- \rightarrow Re_6S_6Cl_8^{2-} + Re_6S_4Cl_{10}$$

Note that both reactions, activated thermally, yield the thermodynamically most stable cluster form, $[Re_6S_6Cl_8]^{2-}$.[19] Note also that the low yields obtained during this preparation of $(Bu_4N)_2[Re_6S_6Cl_8]$ are associated with the small amounts of trivalent anion formed during the solid-state synthesis and with the stoichiometry of the latter disproportionation reaction.

All new tetraalkylammonium salts are soluble in organic solvents such as acetone, $CH_3CN$, THF, and DMF, their solubility increasing with the anion charge. Thus, they are currently engaged in electrocrystallization experiments to give a variety of electroactive cation radical salts.[8-10] Clearly, this unprecedented series of isostructural and isoelectronic molecular anions offers a unique opportunity for many combinations and variations of the structures and properties of such molecular cation radical salts or alloys. In that respect, the synthesis of the neutral molecular forms $[Re_6S_4Cl_{10}]$ and $[Re_6S_5Cl_8]$ is also of great interest. The former molecular solid proved to be insoluble in common solvents. Conversely, the latter linear-chain inorganic polymer was readily soluble in DMF to give the solvated crystalline phase $[Re_6S_5Cl_8(DMF)]\cdot 2.5DMF$. It is of interest to note that we have obtained $(Bu_4N)[Re_6S_5Cl_9]$, identified by the determination of its unit cell, by addition of $(Bu_4N)Cl$ to DMF solutions of $[Re_6S_5Cl_8]$.[20] This is another route to these cluster anions as reported concomitantly by Holm et al. for the selenium series.[7]

**Crystal Structures.** The mode of packing in each crystal structure is shown in the stereoviews of their unit cells.[21] Note that $Re_6S_4Cl_{10}$ is isostructural with $Re_6Se_4Cl_{10}$ and $Re_6S_4Br_{10}$.[22] The structure of $Rb[Re_6S_5Cl_9]$ is different from that of $K[Re_6Se_5Cl_9]$, which was found to crystallize in the cubic space group $Pn\bar{3}$.[16] It also proved to differ from, and appears much densier than, that suggested earlier[16] for $Rb[Re_6S_5Cl_9]$ on the basis of X-ray powder data by analogy with that of $K[Re_6Se_5Cl_9]$. On the other hand, $Rb[Re_6S_5Cl_9]$ appears to be isostructural with $K[Re_6S_5Br_9]$.[23] Note, finally, that the triclinic unit cells of the linear inorganic polymers $[Re_6S_5Cl_8]$, reported here, and $[Re_6Se_5Cl_8]$[24] are different.

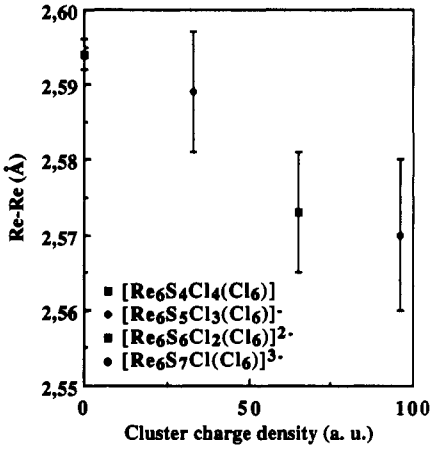


**Figure 2.** Variation of the Re–Re bond distances upon successive sulfur atom addition to the cluster core.

**Structural Correlations: Core Contraction within a Net Cluster Expansion.** The molecular cluster motifs, shown in Figure 1, adopt in all compounds the expected geometry,[6] that is, a $Re_6$ octahedron surrounded by a distribution of S/Cl atoms onto its eight, inner face-capping sites with six rhenium-bonded terminal chlorides ($Cl_t$) to complete the fourteen-ligand set of the $Re_6$ unit. The characteristic interatomic distances within the homogeneous series of molecular clusters in compounds **4–7** are given in Table II. Their comparison allows for an appreciation of two major structural modifications of the cluster geometry as one successively adds up to three sulfur atoms to the cluster cores, keeping their total number of electrons (24) constant. To that effect, the intracluster rhenium–rhenium bond distances are plotted in Figure 2 as a function of the charge per effective molecular cluster volume. The latter can be calculated on the basis of an effective molecular radius taken as the mean distance

(18) Note that the addition of $(Bu_4N)Cl$ to a solution of **2** in water yields an orange powder whose recrystallization in a methanol/acetonitrile mixture yields single crystals of $(Bu_4N)_2[Re_6S_6Cl_8]$ (**6**), identified by their unit cell, in addition to an orange microcrystalline powder. The preparation of X-ray-quality single crystals of the latter has yet proven unsuccessful.

(19) Also in agreement with a similar observation in the corresponding selenium series.[7]

(20) Note that this synthesis of the discrete cluster monoanion from the neutral linear-chain polymer is identical to an alternative route to $(Bu_4N)_2[Mo_6Cl_{14}]$, the reaction of 1 equiv of $(Bu_4N)Cl$ with ethanol solutions of the linear-chain polymer anion $NaMo_6Cl_{13}$: Boubekeur, K.; Perrin, C.; Batail, P. *Acta Crystallogr., Sect. C*, to be submitted for publication.

(21) The stereoviews are available as supplementary material.

(22) Leduc, L.; Perrin, A.; Sergent, M.; Le Traon, F.; Pilet, J. C.; Le Traon, A. *Mater. Lett.* **1985**, *3*, 209. Note that the crystal structure of $Re_6Se_4Cl_{10}$ reported in this paper is described in a nonconventional unit cell setting. The following transformation, applied to the latter, enables the comparison with that of $Re_6S_4Cl_{10}$ reported here: (100, 001, $0\bar{1}0$)

(23) Slougui, A.; Perrin, A.; Sergent, M. *Acta Crystallogr.* **1992**, *C48*, 1917. Again, one should apply the following transformation to obtain a conventional unit cell setting suitable for a ready comparison of the two structures: (101, 010, $\bar{1}00$).

(24) Perrin, A.; Leduc, L.; Sergent, M. *Eur. J. Solid State Inorg. Chem.* **1991**, *28*, 919.

**Table III.** Ranges and Mean Values of Interatomic Distances (Å) in the Neutral Cluster Molecule $Re_6S_5Cl_8$, **4** and $RbRe_6S_5Cl_9$ **1**

| | | $(Re_6S_5Cl_3)Cl_{t4}(Cl_b)_{2/2}$ | $Rb[(Re_6S_5Cl_3)(Cl_t)_6]$ |
|---|---|---|---|
| Re–Re | mean | 2.596(7) | 2.594(4) |
| | range | 2.586(1)–2.607(4) | 2.589(1)–2.599(1) |
| Re–L | mean | 2.421(21) | 2.416(14) |
| | range | 2.384(5)–2.466(5) | 2.391(3)–2.439(3) |
| Re–$Cl_t$ | mean | 2.324(6) | 2.358(7) |
| | range | 2.319(4)–2.330(6) | 2.352(3)–2.365(4) |
| Re–$Cl_b$[a] | mean | 2.458[b] | |
| $(Re\cdots Re)_{trans}$ | mean | 3.672(16) | 3.669(2) |
| | range | 3.648(1)–3.683(1) | 3.667(1)–3.671(1) |

[a] b for bridging chlorine, common to two cluster molecules in the solid. [b] Mean over two half-cluster molecule values (2.457(4)–2.458(5)) in the asymmetric unit.

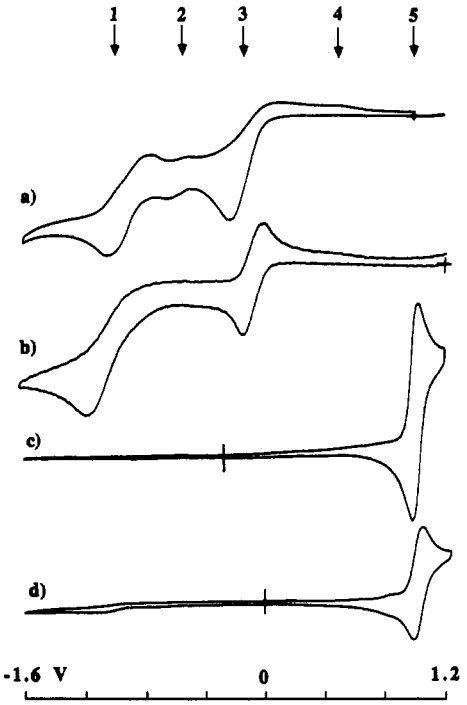


**Figure 3.** Cyclic voltammograms at a platinum electrode, vs SCE in acetonitrile containing 0.1 M $(Bu_4N)PF_6$ (scan rate 0.1 V $s^{-1}$), of (a) $[Re_6S_5Cl_8(DMF)]$, (b) $(Bu_4N)[Re_6S_5Cl_9]$, (c) $(Bu_4N)_2[Re_6S_6Cl_8]$, and (d) $(Bu_4N)_3[Re_6S_7Cl_7]$.

from the center of the cluster to the outer terminal chlorine, $Cl_t$. The salient, striking effect is a contraction of the hexanuclear rhenium octahedron (Figure 2a). Note, however, that this contraction is not regular throughout the series but presents a discontinuity upon going from the $S_5Cl_3$ to $S_6Cl_2$ core ligand distribution. Another noteworthy feature (Table II) is a smoother continuous increase of the Re–$Cl_t$ interatomic distances. It is of interest to recognize that the inner cluster core contraction occurs while the net volume of the cluster molecule increases by ca. 4.5% throughout this series of isoelectronic, electron-precise (24e) species.

The characteristic interatomic distances for the cluster molecules in **1** and **3** are given in Table III. Similar correlations within the homogeneous series of rubidium salts will have to await the synthesis and structure of $Rb_2[Re_6S_6Cl_8]$ and $Rb_3[Re_6S_7Cl_7]$.

**Electrochemistry. Redox Processes.** The observed discontinuity in the cluster core structures of $[Re_6S_5Cl_9]^-$ and $[Re_6S_6Cl_8]^{2-}$ is also apparent in their redox properties. The cyclic voltammograms of the molecular cluster salts $(Bu_4N)[Re_6S_5Cl_9]$, $(Bu_4N)_2[Re_6S_6Cl_8]$, $(Bu_4N)_3[Re_6S_7Cl_7]$, and $[(Re_6S_5Cl_3)Cl_5(DMF)]$ were recorded in acetonitrile. As shown in Figure 3, two strikingly different types of electrode processes are identified, depending upon the number of chalcogen atoms within the cluster cores. Thus, the cyclic voltammograms of $[(Re_6S_5Cl_3)Cl_5(DMF)]$ and $(Bu_4N)[(Re_6S_5Cl_3)Cl_6]$ (Figure 3a,b), with identical cluster cores, exhibit a first reduction process (3) (Table IV), nonreversible (solvent dependent) for $[(Re_6S_5Cl_3)Cl_5(DMF)]$ and quasireversible for $(Bu_4N)[(Re_6S_5Cl_3)Cl_6]$, followed by a broader nonreversible additional reduction (1). On the return scan, a broad oxidation (4) is observed which proved to be associated with the former nonreversible reduction (1) since it is not present on restricted scans (Figure 3). Note that an additional nonreversible process (2) is observed in the cyclic voltammogram of $[Re_6S_5Cl_8(DMF)]$ (Figure 3a). Clearly, the appearance of this extra cathodic process is a characteristic electrochemical feature of the complexed cluster core by comparison with the cyclic voltammogram of the pristine salt $(Bu_4N)[Re_6S_5Cl_9]$ shown in Figure 3b.[25]

**Table IV.** Voltammetric Process Potentials $E°$, V ($\Delta Ep$, mV), for **8**, **5**, **6** and **7**

| | 1 | 2 | 3 | 4 | 5 |
|---|---|---|---|---|---|
| $Re_6S_5Cl_8(DMF)$ | –0.89 | –0.58 | –0.30 | 0.50 | |
| $(Bu_4N)Re_6S_5Cl_9$ 2–/1– | –0.93 | | –0.075 (90) | 0.35 | |
| $(Bu_4N)_2Re_6S_6Cl_8$ 2–/1– | | | | | 0.99 (75) |
| $(Bu_4N)_3Re_6S_7Cl_7$ 3–/2– | | | | | 1.02 (75) |

The cyclic voltammograms of $(Bu_4N)_2[Re_6S_6Cl_8]$ and $(Bu_4N)_3[Re_6S_7Cl_7]$, shown in Figure 3c,d, are markedly different from those of the former cluster compounds. Indeed, one reversible oxidation is observed at ca. 1.0 V for both compounds, with no indication for any reduction process. The voltammograms of both compounds are essentially identical but for the presence of a very weak precursor process for **7**.

The quasireversible redox processes for the molecular cluster anions $[Re_6S_{4+n}Cl_{10-n}]^{n-}$ ($n$ = 1–3) are summarized as follows:

$$[Re_6S_5Cl_9]^- \underset{-e^-}{\overset{+e^-}{\rightleftarrows}} [Re_6S_5Cl_9]^{2-}$$

$$[Re_6S_6Cl_8]^{2-} \underset{+e^-}{\overset{-e^-}{\rightleftarrows}} [Re_6S_6Cl_8]^-$$

$$[Re_6S_7Cl_7]^{3-} \underset{+e^-}{\overset{-e^-}{\rightleftarrows}} [Re_6S_7Cl_7]^{2-}$$

**Electrochemical Monitoring of the $[Re_6S_5Cl_9]^-$ + $(Me_3Si)_2S$ Reactions.** Such a clear-cut crossover in the redox properties of the molecular clusters upon an increase of one sulfur in the cluster core provides a unique opportunity to monitor the cluster core reactions upon addition of $(Me_3Si)_2S$ to acetonitrile solutions of $[Re_6S_5Cl_9]^-$. The evolution of the cyclic voltammogram of $(Bu_4N)[Re_6S_5Cl_9]$ upon addition of an excess (ca. 3 equiv) of $(Me_3Si)_2S$, followed by the addition of $PPh_4Cl$, is shown in Figure 4. The *concomitant* diminution of the reduction peak (3), characteristic of $[Re_6S_5Cl_9]^-$, and the emergence of the oxidation peak (5) are clear indications of the formation of either $[Re_6S_6Cl_8]^{2-}$ or $[Re_6S_7Cl_7]^{3-}$ or both, thereby demonstrating the reactivity of the cluster core toward sulfur in the solution phase.

**Summary.** Searching the Rb–Re–S–Cl system for soluble salts of molecular, discrete forms of octahedral $Re_6$ cluster anions, in which different S/Cl proportions in the inner cluster cores are associated with a variety of cluster charges, we have synthesized and determined the structure of single crystals of $Rb[Re_6S_5Cl_9]$ and $(Rb^+)_5[Re_6S_6Cl_8^{2-}][Re_6S_7Cl_7^{3-}]$ as well as single crystals of

(25) Note that the cyclic voltammogram of $(Bu_4N)[Re_6S_5Cl_9]$ is essentially identical to that of $(Bu_4N)[Re_6Se_5Cl_9]$.[2]

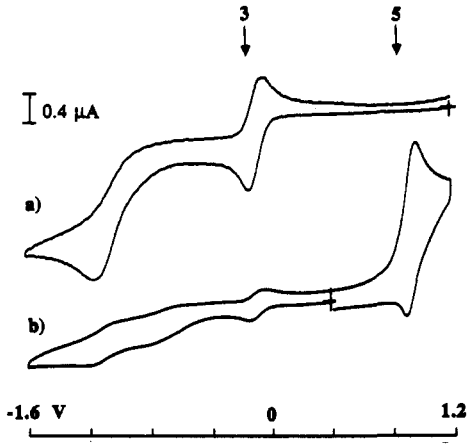


**Figure 4.** Cyclic voltammograms at a platinum electrode, vs SCE in acetonitrile containing 0.1 M $(Bu_4N)PF_6$ (scan rate 0.1 V $s^{-1}$), of $(Bu_4N)[Re_6S_5Cl_9]$ (a) before and (b) after addition of $(Me_3Si)_2S$ and $PPh_4Cl$. Note that the reversible oxidation (5) characteristic of $[Re_6S_6Cl_8]^{2-}$ or/and $[Re_6S_7Cl_7]^{3-}$ (Figure 3c,d) is superposed in (b) with the broader, nonreversible oxidation of $Cl^-$.

the molecular phase $[Re_6S_4Cl_{10}]$ and of the neutral linear-chain polymer $[Re_6S_5Cl_8]$.

It is demonstrated that $Rb[Re_6S_5Cl_9]$ is soluble at ambient temperature in ethanol, from which $(Bu_4N)[Re_6S_5Cl_3(Cl_6)]$ precipitates by addition of $(Bu_4N)Cl$. The same procedure conducted in hot solvents gives $(Bu_4N)_2[Re_6S_6Cl_2(Cl_6)]$ instead, which contains the thermodynamically most stable inner cluster form. Also of great interest is the synthesis of the new (24e) cluster core $[Re_6S_7Cl]^{3+}$ in $(Bu_4N)_3[Re_6S_7Cl(Cl_6)]$ by adding $(Bu_4N)Cl$, specifically to the water solution used to wash solid $Rb[Re_6S_5Cl_9]$ at room temperature or in cold water even. This demonstrates that significant amounts of water-soluble $Rb_3[Re_6S_7Cl_7]$ are obtained along with $Rb[Re_6S_5Cl_9]$ during the high-temperature solid-state synthesis, in agreement with the observed extreme water solubilty of $(Rb^+)_5[Re_6S_6Cl_8^{2-}][Re_6S_7Cl_7^{3-}]$ crystals.

In addition, $[Re_6S_5Cl_8]$ is highly soluble in DMF and the neutral solvated cluster $[Re_6S_5Cl_8(DMF)]$ has been prepared. Addition of $(Bu_4N)Cl$ to DMF solutions of $[Re_6S_5Cl_8]$ provides an alternative route to $(Bu_4N)[Re_6S_5Cl_9]$.

Analysis of structural correlations in the unique series of crystal structures of $[Re_6S_4Cl_{10}]$ and $(Bu_4N)_n[Re_6S_{4+n}Cl_{10-n}]$ ($n = 1-3$) reveal a contraction of the cluster core upon addition of sulfur atoms. This contraction is not regular but is more pronounced between the $[Re_6S_5Cl_3]^{5+}$ and $[Re_6S_6Cl_2]^{4+}$ cluster cores. This discontinuity is also observed in the redox properties of the series of cluster anions, $[Re_6S_6Cl_8]^{2-}$ and $[Re_6S_7Cl_7]^{3-}$ being reversibly oxidized (at ca. 1.0 V vs SCE) to the corresponding paramagnetic (23e) species.

**Acknowledgment.** We thank A. Perrin for experimental assistance in our preliminary synthesis of $Rb[Re_6S_5Cl_9]$.

**Supplementary Material Available:** Stereoviews, atom-numbering figures, and listings of positional and thermal parameters and interatomic distances and angles for compounds in Table I (83 pages). Ordering information is given on any current masthead page.